VOLUME 28, 2, 217–224
ASLE TRANSACTIONS

Eccentricity Measurements on a Tilting-Pad Bearing©

HARLEY TRIPP and BRIAN MURPHY*
Shell Development Company
Houston, Texas 77001

This paper describes an experimental apparatus and procedure for measuring steady-state eccentricities in journal bearings. Eccentricity measurements for two five-pad tilting-pad bearings with load-on-pad and preloads of 0.0 and 0.2 are presented. Good agreement is shown between measured and theoretical eccentricities for a range of Sommerfeld numbers between 0.2 and 3.0. Relatively small deviations of the journal center from the load axis indicate negligible cross-coupling effects were present in the bearings.

INTRODUCTION

This paper presents experimentally determined steady-state operating eccentricities of a shaft operating in a five-pad tilting-pad bearing, with load on pad. Although measurements showing eccentricities of a shaft operating in a circular journal bearing have been widely published (*1*), (*2*), measurements showing eccentricities in tilting-pad bearings are almost nonexistent in engineering literature. As a result, questions exist not only about the accuracy of calculated tilting-pad bearing characteristics, but also about the existence of cross-coupling effects in these bearings.

DESCRIPTION OF THE TEST APPARATUS

The apparatus used for measuring the bearing characteristics, shown in Fig. 1, consists of a 1.28 meter (50.5 in) long uniform rotor 98.4 mm (2.5 in) in diameter, supported by tilting-pad bearings mounted near each end of the shaft. The bearing pads each have a concave seat that rests on a hemispherical support that allows the pad to pivot with respect to the housing. Figure 2 shows the basic concept of this type of pad support. In addition, the bearing housing rests in a spherical seat within the bearing pedestal which permits angular motion of the housing in the pedestal. This helped accommodate static misalignment between the shaft and bearing pedestal. Once the desired alignment had been achieved, the bearing was clamped in place to prevent additional motion of the housing in the pedestal. The rotor was connected through a flexible coupling to a layshaft, which was supported by two additional tilting-pad bearings. The layshaft was belt-driven by a 22.4-KW (30-hp) variable-speed electric motor.

The outboard bearing was used as the test bearing. Two bearings, having the dimensions shown in Fig. 3, but having slightly different shaft-to-bearing clearances, were tested. Before the test apparatus was assembled, the radius of curvature of each bearing pad was checked using a 63.58 mm (2.504 in) diameter mandrel. Pads with different radii were reground to the desired curvature. The shaft-to-bearing radial clearance for the first bearing was then set to 0.5 mm (0.002 in) by grinding the spacer shims behind each hemispherical pad support (note: all stated clearances are in line with the pad pivot). Since a 63.58 mm (2.500 in) diameter shaft was used, this resulted in nominal preload of 0.0, and is hereafter referred to as the nonpreloaded bearing. The clearance of the second bearing was set slightly smaller so tests could be performed on a preloaded bearing. Each test bearing had an axial length of 25.4 mm (1.0 in), which corresponds to a L/D ratio of 0.4.

Clearance measurements (described in the next section) performed after each set of eccentricity measurements showed that the nonpreloaded bearing had an actual radial bearing clearance of 0.056 mm (0.0020 in) and the preloaded bearing had a radial clearance of 0.043 mm (0.0016 in), which corresponds to a 0.2 preload. These numbers were used in presenting the measured data although they varied slightly from run to run.

The total weight of the test shaft was 34.0 kg (75 lb). The portion of this weight supported by the test bearing was measured as 19.0 kg (42 lb) using a strain-gauge-type load cell mounted in place of the test bearing pedestal. The same load cell was used to calibrate additional external loads which were applied to the bearing through two pairs of plastic rollers running on the shaft just inboard and outboard of the test bearing, as shown in Fig. 4. The rollers were mounted in yokes which, in turn, were forced down by air cylinders.

*Present address: Rocketdyne Corp.

Presented at the 39th Annual Meeting in Chicago, Illinois, May 7–10, 1984
Final manuscript accepted May 17, 1984

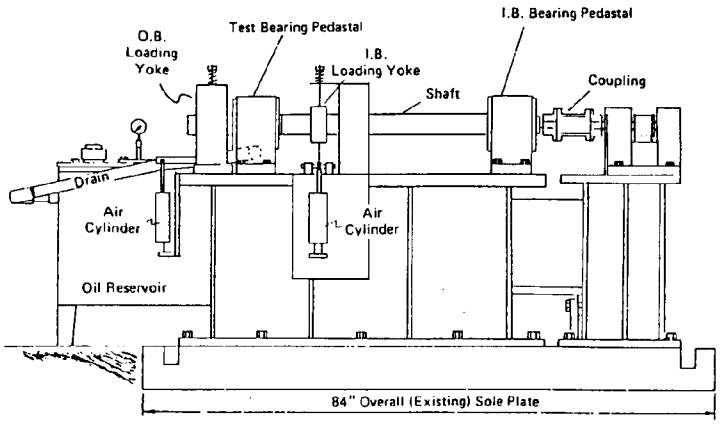

Fig. 1—Rotor/bearing apparatus as modified for measuring tilting-pad bearing characteristics

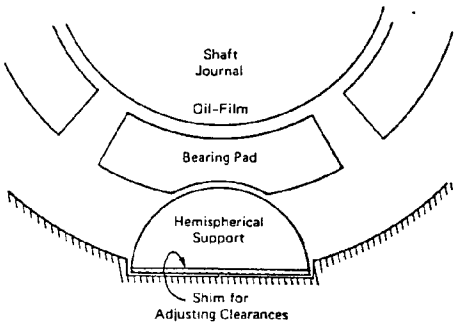

Fig. 2—Basic concept of support for tilting pad

Lever arms connecting the air cylinders to the yokes were adjusted, so that equal portions of bearing load were applied to the bearing by each yoke for the same air pressure.

The shaft location relative to the bearing pedestal was measured using eight noncontact eddy current proximity probes, mounted in orthogonal pairs 25.0 mm (1.0) in inboard and outboard of each end of the test bearing (see Fig. 4). The voltage output of these probes was 8.0 volts dc per mm (0.04 in) of clearance between the probe tip and the surface of the shaft. Steady-state shaft positions were obtained by using low-pass filters to remove the dynamic component of the probe signals, leaving only the static voltages representing the steady-state shaft position. Measurements of probes directly opposite each other were combined so that the average difference between the probes gave the relative shaft position with respect to the probe tips, while canceling the effect of uniform thermal expansion of the shaft and/or bearing-pedestal housing. Data from both ends of the bearing were averaged to determine the shaft position at the axial midplane of the bearing.

A light turbine oil with a viscosity of 19.6 cp @ 48.9°C (120°F) was used as the bearing lubricant. Determining the oil-film temperatures was a major problem. Direct measurements of the actual oil-film temperatures are complex (*3*) and beyond the scope of this work. As an indirect means of measuring this temperature, thermocouples were installed in three locations: (1) in the oil supply line at the bearing inlet, (2) in the oil stream flowing out of the trailing edge of the loaded pad, and (3) at the oil exit from the bearing. For the preloaded bearing only, a fourth thermocouple was implanted in the babbitt of the loaded pad to monitor bearing babbitt temperature.

Shaft position, oil temperatures, external load, and rotor speed were monitored and recorded using a data acquisition system in conjunction with a small desktop computer. This system allowed the accumulation of 30 individual measure-

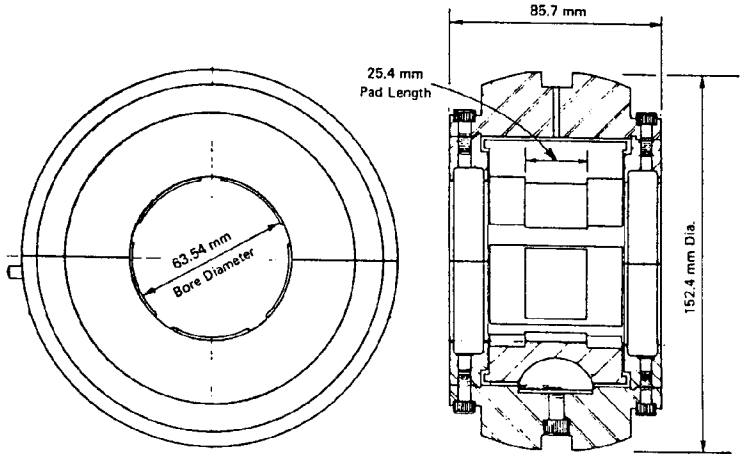

Fig. 3—Engineering drawings of the special test bearing used for eccentricity measurements

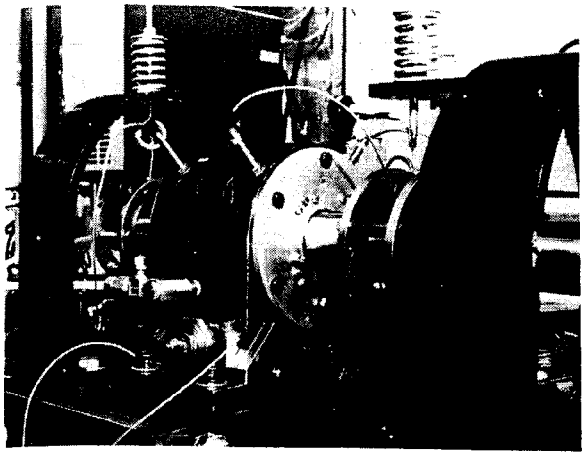

Fig. 4—The rollers and yoke used to load the journal and bearing

ment points per second. Reducing and presenting the data took an additional two seconds. Tabulated results were printed using an online computer printer, and the shaft eccentricity locations were plotted using a *x-y* digital plotter.

TEST PROCEDURE

A complete set of measurements was taken using the nonpreloaded bearing and then repeated using the preloaded bearing. The measurements discussed here were taken with the load centered over the bottom bearing pad. For each test series, a set of measurements was first taken with the shaft rotating counterclockwise, and then repeated with the shaft rotating clockwise. This reduced errors due to asymmetry in the bearing and in the loading. Typical results showing the data recorded at 2000 rpm for the nonpreloaded bearing are shown in Fig. 5.

Since thermal expansion of the bearing housing, which supported the probes, made it difficult to define the center of the bearing, steady-state shaft eccentricities were measured with respect to a lightly loaded equilibrium position as defined with the shaft rotating at 8500 rpm with no additional external load. This lightly loaded equilibrium position was identified after thermal equilibrium had been established, but before eccentricity measurements were made for each test. The Sommerfeld number for this lightly loaded equilibrium position is 10.8, which corresponds to an eccentricity ratio of less than 0.05 (*4*). Measurements also showed that this position approximated the bearing center. At the end of each test run, after the rotation had stopped, the bottom and top locations of the bearing were defined by forcing the shaft down and then up with a 43.5-kg (100-lb) load, and measuring the resulting shaft movement. These measurements were used to determine the shaft-to-bearing clearance, and to be sure that the lightly loaded equilibrium position approximated the bearing center.

Data were recorded only after thermal equilibrium of the bearing oil had been achieved at each test condition. At each test point, the oil supply pressure, and thus the oil flow through the bearing, was regulated as a means of controlling the oil temperature. In most cases, this temperature was maintained between 42.2° and 43.3°C (108° and 110°F),

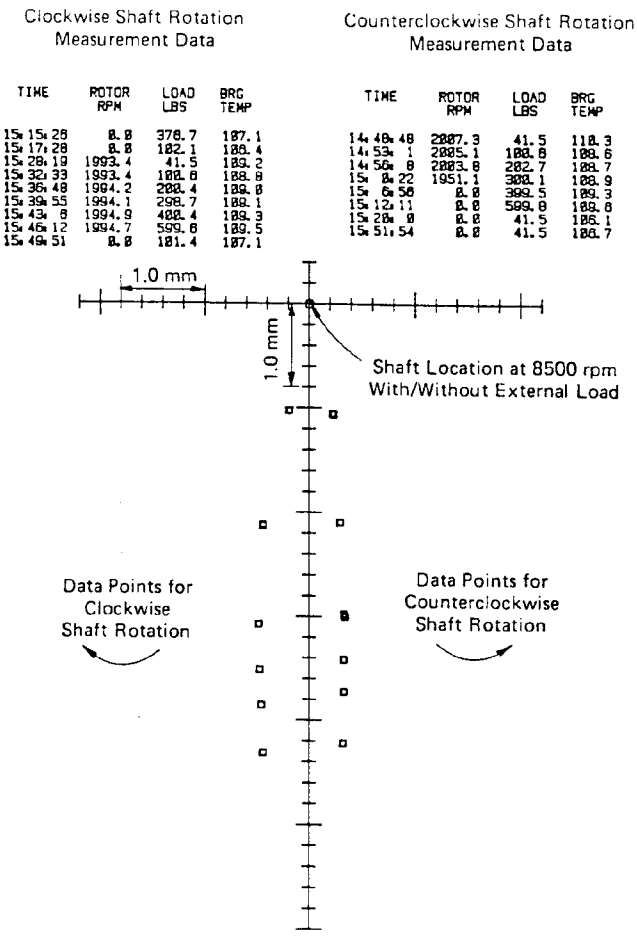

Fig. 5—Actual shaft eccentricity measurements recorded at 2000 rpm, with various external bearing loads. Each measurement location represents three data points.

but at the extremely high and low bearing load test conditions, the temperature exceeded these limits.

Four test series were run for each bearing, with each series consisting of four to six test conditions. Each test series included a combination of shaft rotational speeds and bearing loads representing the same five Sommerfeld numbers shown in Table 1. The test series were designed to reproduce Sommerfeld numbers between 0.2 and 1.0. Measurements using the 19.0-kg shaft weight at various speeds extended the range of individual measurements to a Sommerfeld number of 3.0. This range of Sommerfeld numbers (0.2 to 3.0) corresponds to turbomachinery bearings typically used in the petrochemical industry where bearing radius/clearance ratios are approximately 0.001 to 0.002, speeds range from 3000 to 10 000 rpm, and unit bearing loads range from 138. $\times 10^4$ to 207 $\times 10^4$ N/m^2 (200 to 300 lb/in^2).

Test series 1, 2, and 3 were run at constant speeds, with measurements taken using five or six bearing loads. The fourth test series used a constant bearing load of 136 kg, and shaft speeds of 300, 1000, 2000, and 3000 rpm. Three of the four data conditions measured during the fourth test series duplicated speeds and loads of previous test conditions.

TABLE 1—OPERATING CONDITIONS FOR MEASUREMENTS ON TILTING PAD BEARINGS

TEST COND.	1	2	3	4	CALCULATED*	
	1000 rpm	2000 rpm	3000 rpm	136.0 kg	SOMMERFELD NO.	ECCENTRICITY
a	19.0 kg	19.0 kg	19.0 kg	—		
b	—	45.5	68.0		1.0	0.40
c	45.5	90.7	136.0	3000 rpm	0.6	0.45
d	68.0	136.0	204.1	2000 rpm	0.4	0.5
e	90.7	181.4	272.1	1500 rpm	0.3	0.60
f	136.0	272.1	408.2	1000 rpm	0.2	0.65

*Calculations are based on a 43.3°C oil temperature and 0.0 preload.

At each test condition, after thermal equilibrium had been obtained, 15 sets of measurements were taken at 10-second intervals. Each set of measured data consisted of 13 measurements including the shaft position, oil temperature, and shaft speed. After every five measurement sets, a data point representing the average of these five sets was plotted. The statistical standard deviation of the 15 data sets was typically 2.5 μm.

EXPERIMENTAL RESULTS

Results of the test runs showing measured journal center eccentricities for both bearings are presented in Fig. 6 and 7. In these figures, the data points show the shaft position for various operating conditions relative to the shaft equilibrium position as defined at 8500 rpm.

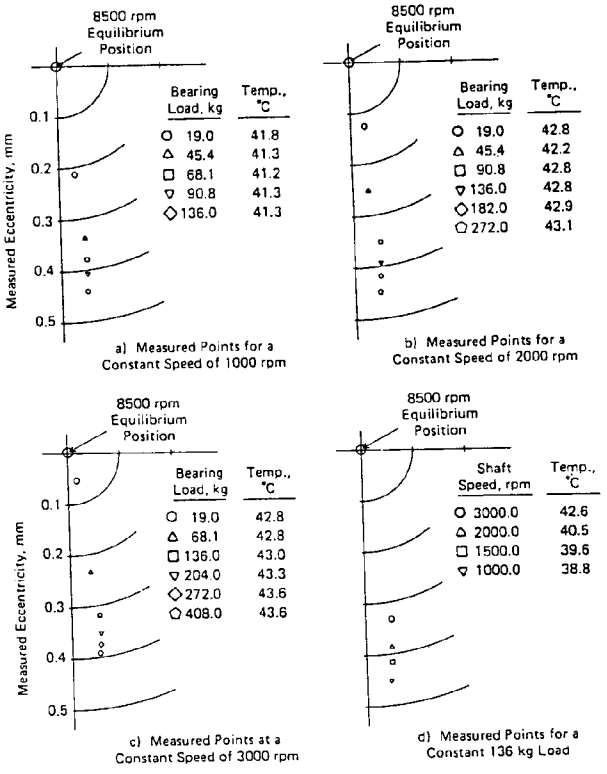

Fig. 6—Steady-state bearing eccentricity measurements for a five-pad, tilting-pad bearing, load on pad, L/D = 0.4. Measurements are for test bearing with no preload.

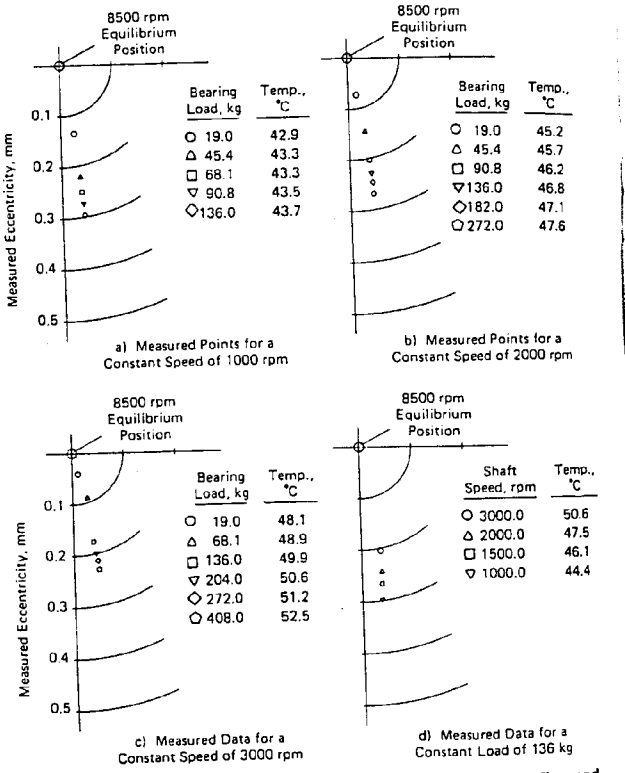

Fig. 7—Steady-state bearing eccentricity measurements for a five-pad, tilting-pad bearing, load on pad, L/D = 0.4, and 0.2 preload.

Each plotted point represents the average value of the 15 data sets measured with counterclockwise shaft rotation and 15 data sets measured with clockwise rotation. The sign of the horizontal offset of the data for clockwise shaft rotation has been reversed so that these data could be averaged with the counterclockwise shaft rotation data.

The measurements in these figures have been corrected for elastic deformation due to the shaft, bearing pad and seat, and bearing housing. Load deflection measurements for the nonrotating shaft showed that for a bearing load of 227 kg (500 lb), the shaft deflected 0.01 mm (0.0005 in) at the probe measurement locations. (i.e., an ensemble stiffness of 1 000 000 lb/in).

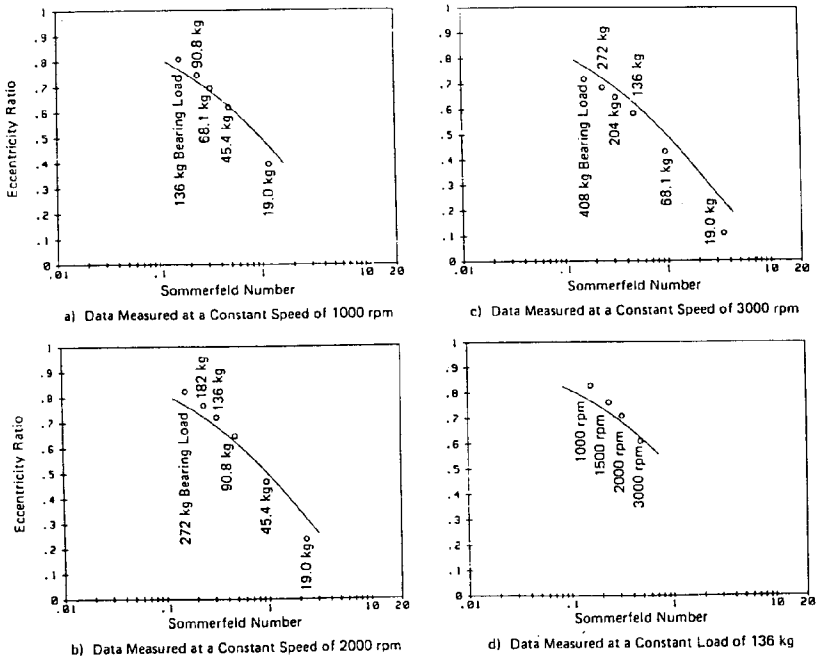

Fig. 8—A comparison of points showing measured steady-state bearing eccentricities and the solid line showing theoretical eccentricities for a five-pad, tilting-pad bearing, with load on pad, L/D = 0.4, and 0.0 preload.

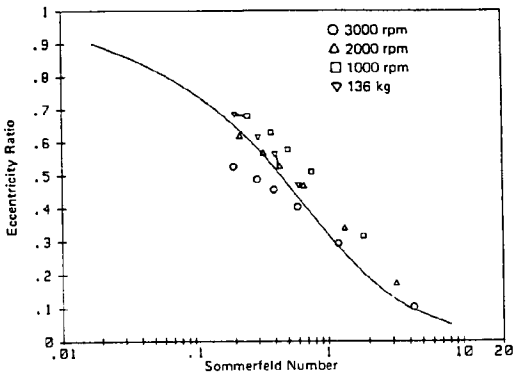

Fig. 9—A summary of measured eccentricities, shown by the data points, and the theoretical points, represented by the solid line for a five-pad, tilting-pad bearing, with load on pad, L/D = 0.4, and a preload of 0.0.

DISCUSSION OF RESULTS

Bearing eccentricity measurements, such as shown in Figs. 6 and 7, are usually normalized and plotted as a function of the total bearing clearance. However, problems in defining the bearing center and clearances made this type of presentation more attractive.

Measured eccentricity ratios are shown as a function of the Sommerfeld number in Figs. 8–11. In these figures, the data points represent measured eccentricities as a function of the corresponding Sommerfeld numbers calculated using measured clearances and oil temperatures. The Sommerfeld numbers corresponding to the measured data in Fig. 9 are based on the oil viscosity corresponding to the temperature of the oil coming off the trailing edge of the loaded pad. The numbers in Fig. 11 are based on the viscosity corresponding to the bearing pad temperature. The solid line represents the theoretical locus based on results from the computer program discussed in Ref. (*4*).

The average value of the absolute differences between the measured and calculated eccentricities is 4.2 percent. The largest difference between the measured and calculated data is 14.8 percent.

Differences between measured and calculated results can be attributed to difficulties in defining the bearing center, the bearing clearances, and the oil viscosity. The spread of the measurement error can be estimated by the connected points in Figs. 9 and 11. These points connected by a line are the three test conditions duplicated by measurements in test number 4. In Fig. 11, all of these points either touch or coincide with each other. With the exception of the 3000 rpm data, the identical speed/load points in Fig. 9 show very good agreement.

As shown in Figs. 5–7, all of the measured data deviate slightly from the bearing vertical centerline. Figure 12 shows a continuous locus curve of shaft centers for a shaft rotating at 3000 rpm. This curve consists of 100 individual data points recorded as the bearing load was gradually increased from 42 to 584 lb. This load range approximates Sommerfeld numbers between 0.3 and 3.0. The constant, almost linear deflection of the curve from the vertical load axis results from cross-coupling stiffness within the tilting-pad bearing. In the plotted range, the deflection from the vertical axis is about 10 percent of the vertical or principle change resulting from increased vertical loads. This indicates the cross-coupling stiffness coefficients in this direction are one order of magnitude smaller than the principle stiffness coefficients.

The direction of deviation from the vertical axis is consistent with that in a plain cylindrical fluid film bearing,

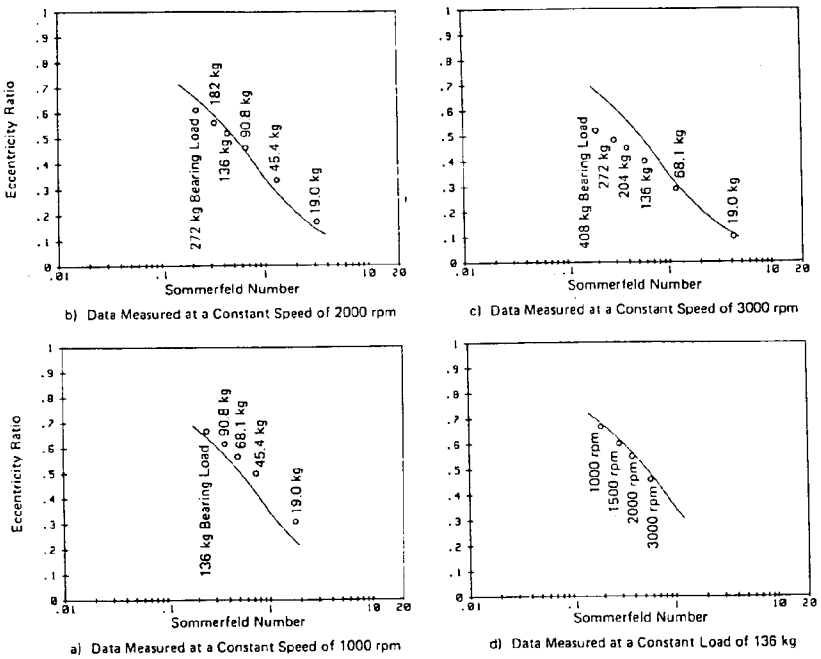

Fig. 10—A comparison showing measured steady-state bearing eccentricities, represented by points, and the theoretical curve for a five-pad, tilting-pad bearing, with load on pad, L/D = 0.4, and a 0.2 preload.

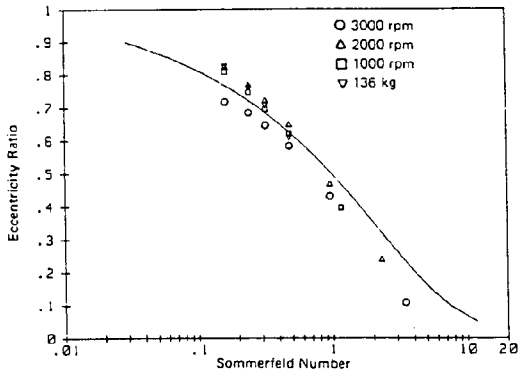

Fig. 11—A summary showing measured eccentricities, shown by the data points, and the theoretical curve for a five-pad, tilting-pad bearing, load on pad, with L/D = 0.4, and a 0.2 preload. Measurements are for a test bearing with 0.2 preload.

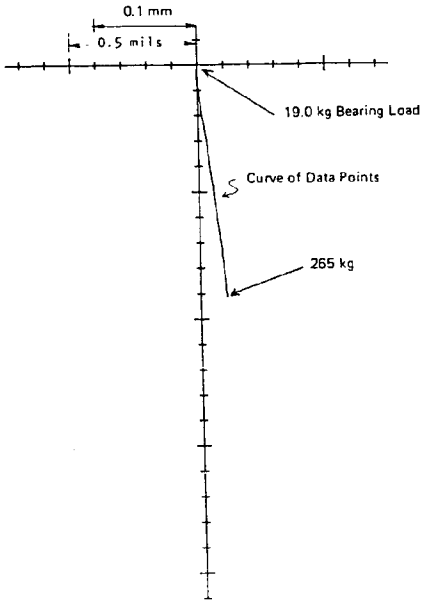

Fig. 12—A measured locus curve of steady-state shaft centers for a shaft rotating counterclockwise at 3000 rpm. This curve consists of 100 data points recorded as the bearing load was gradually increased from 19.0 to 265 kg.

indicating the sign of the cross-coupling stiffness is the same as that in a plain cylindrical bearing.

CONCLUSIONS

In general, measured eccentricities show good agreement with the calculated eccentricities. This indicates that the accuracy of tilting-pad bearing stiffnesses calculated using existing technology is within the accuracy of bearing clearance measurements normally encountered in large turbomachinery for the case of a bearing loaded on one pad.

These measurements also confirm that only minimal cross-coupling stiffness exists in tilting-pad bearings. Until other calculation techniques are improved, the usual practice of ignoring these terms in rotor dynamics calculations dealing with tilting-pad bearings appears to be acceptable.

REFERENCES

(1) Orcutt, F. K. and Arwas, E. B., "The Steady State and Dynamic Characteristics of a Full Circular Bearing and a Partical Arc Bearing in the Laminar and Turbulent Flow Regimes," *J. Lubr. Tech. Trans. of the ASME*, **89,** pp 143–152 (April 1967).

(2) Tonnesen, J. and Hansen, P. K., "Some Experiments of the Steady State Characteristics of a Cylindrical Fluid-Film Bearing Considering Thermal Effects," *J. Lub. Tech. Trans. of the ASME*, **1,** pp 107–114 (Jan. 1981).

(3) DeChoudhury, P. and Masters, D. A., "Performance Tests of Five-Shoe Tilting-Pad Journal Bearing," *ASLE Trans.*, **27,** pp 61–66 (1984).

(4) Nicholas, J. C., Gunter, E. J. Jr., and Allaire, P. E., "Stiffness and Damping Coefficients for the Five-Pad Tilting-Pad Bearing," *ASLE Trans.*, **22,** 2, pp 113–124 (1979).

DISCUSSION

F. A. MARTIN (Member, ASLE)
Glacier Metal Company Ltd.
Wembley, Middlesex HA0 1HD England

The authors are to be commended for their experimental work which is always welcome in this computer age, where the bias nowadays is generally towards a theoretical approach.

Our experience in predicting dynamic coefficients (*A1*), relating particularly to the authors' discussion on cross-coupled stiffness and attitude angle for a five-pad bearing is as follows:

(a) *With the load on the pad* ($\beta = 0$, see Fig. A1) the cross-coupled coefficients are extremely small and are negligible compared with the direct coefficients.

(b) *When allowing for pad inertia* (assuming pad frequency is synchronous with shaft rotational frequency)—this generally has only a marginal effect on the coefficients under typical operating conditions.

(c) *Considering different temperatures on each pad* (rather than using a global temperature) can have a significant effect on the XX coefficients (notation, Fig. A1) although the cross coefficients are still negligible.

(d) *Altering load angle* β *relative to the pivot position* will have a significant effect on the cross-coupled stiffness (as well as on the direct values) especially when the pivot positions are asymmetric about the load line. Such conditions might occur in practice if the load position is not precisely known and in particular when the load is influenced by gear tooth loading as well as the static weight of the rotor. Figure A2 relates to the authors bearing with a load of 1335 N (300 lbf), a speed of 3000 rev/min and preset of zero. The theory used allows for different temperatures on each pad and although this has some influence on the stiffness coefficients, the significant cross-coupled stiffness for this case appear mainly as a result of the asymmetry of forces from each pad.

The predicted attitude angles for cases (a), (b), and (c) above are extremely small and can generally be considered as zero. For case (d), even when the cross-coupled stiffnesses are relatively large, the predicted attitude angles are only a few degrees (about 3.5 degrees with a preset of 0.2).

It is hoped that this discussion, particularly relating to asymmetric loading and resulting cross coefficients, will form a useful supplement to the authors' paper.

REFERENCE

(*A1*) Jones, G. J. and Martin, F. A., "Geometry Effects in Tilting-Pad Journal Bearings," *ASLE Trans.*, **22**, 3, pp 227–244 (1979).

AUTHORS' CLOSURE

The authors wish to thank F. A. Martin for his contribution. In particular, we appreciate his discussion on the relative merits of a variety of effects which can possibly generate cross-coupled stiffness in the five-pad bearing. On the whole, we concur on all points as he has presented them. We, in fact, considered the possibility that different oil film temperatures on each pad could produce at least a portion of the observed cross-coupling, but our bearing analysis computer program (*4*) could not readily be used to inves-

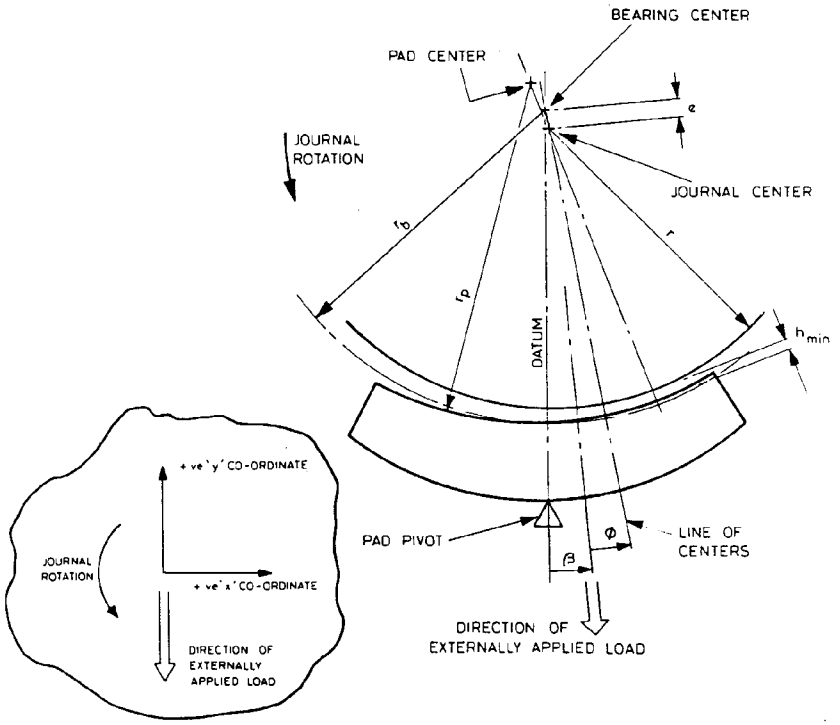

Fig. A1—Bearing notation

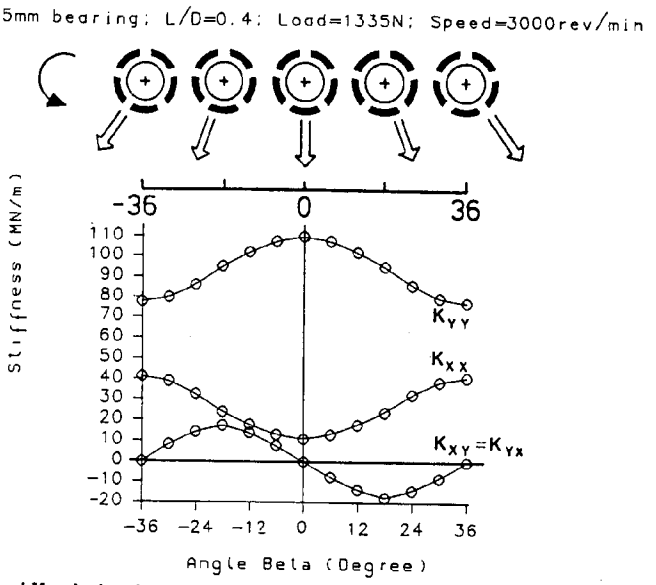

Fig. A2—Predicted stiffness for Tripp and Murphy bearing

tigate this. The effect of pad inertia on cross-coupled stiffness is well known and documented, and we, as well, judged this effect to be minimal. As to the effect of altering the applied load angle, we feel that the air cylinder-rollers loading system provided a consistent load angle directed through the bottom pad pivot. An important note on this point is brought out by Fig. A2. Assuming that the observed cross-coupled stiffness is caused by a nonzero load angle, the resulting horizontal deflection of the journal should be in the same direction regardless of the direction of rotation. Figure 5 showed that the horizontal deflection of the test apparatus reversed when the rotation is reversed (recall the flexible coupling drive arrangement). For this reason, the authors feel that other, as yet unforeseen, factors need be identified and investigated to adequately explain the observed levels of cross-coupled stiffness.

One other note brought out by the data of Fig. A2 concerns the rotordynamic influence of cross-coupled stiffness of the variety such as due to nonzero load angles. Of interest here is the direct effect on rotordynamic stability. For this case, the stiffness coefficients K_{xy} and K_{yx} are equal in *both* magnitude and sign. In practical cases, this class of cross coupling is not destabilizing (recall that $K_{xy} = -K_{yx}$ is generally regarded as destabilizing). This point is clearly seen when one computes the energy either added to, or dissipated from, the whirling motion of a rotor on a "per cycle" basis for the stiffnesses K_{xy} and K_{yx}.

$$E = (\pm A)\,(K_{xy} - K_{yx}) \text{ per whirl cycle}$$

Here a positive E is energy addition and would be regarded as destabilizing. The enclosed area of the whirl orbit is A and is taken as positive for counter-clockwise whirl and negative for clockwise whirl. This result is true regardless of the particular shape of the orbit. It is seen that E is identically zero whenever $K_{xy} = K_{yx}$, and there is no direct effect on stability. Note that when $K_{xy} = -K_{yx}$ there is a destabilizing effect on whirl in one direction and a stabilizing effect on whirl in the other direction, as determined by the individual signs of K_{xy} and K_{yx}. This point has been emphasized here for two reasons. First, one should not automatically assume that cross-coupled stiffness is destabilizing. Second, the measurements made with the test apparatus of this article were insufficient to determine which of the above two classes of cross coupling was present. To accomplish this, independent static load-deflection measurements must be made in *two* directions, ideally in the horizontal and vertical directions. This would enable one to then compute the complete set of stiffness coefficients K_{xx}, K_{yy}, K_{xy}, and K_{yx}.